Materials Research Bulletin 45 (2010) 56–62

Contents lists available at ScienceDirect

Materials Research Bulletin

journal homepage: www.elsevier.com/locate/matresbu

Vinyl monomers-induced synthesis of polyvinyl alcohol-stabilized selenium nanoparticles

Chetan P. Shah, Krishan K. Singh, Manmohan Kumar *, Parma N. Bajaj

Radiation and Photochemistry Division, Bhabha Atomic Research Centre, Trombay, Mumbai 400 085, India

ARTICLE INFO

Article history:
Received 29 May 2009
Received in revised form 4 August 2009
Accepted 2 September 2009
Available online 8 September 2009

Keywords:
A. Nanostructure
A. Semiconductor
B. Chemical synthesis
C. Differential scanning calorimetry (DSC)
C. Electron microscopy

ABSTRACT

A simple wet chemical method has been developed to synthesize selenium nanoparticles (size 100–200 nm), by reaction of sodium selenosulphate precursor with different vinyl monomers, such as acrylamide, N,N′-dimethylene bis acrylamide, methyl methacrylate, sodium acrylate, etc., in aqueous medium, under ambient conditions. Polyvinyl alcohol has been used to stabilize the selenium nanoparticles. Average size of the synthesized selenium nanoparticles can be controlled by adjusting concentration of both the precursors and the stabilizer. Rate of the reaction as well as size of the resultant selenium nanoparticles have been correlated with the functional groups of the different monomers. UV–vis optical absorption spectroscopy, X-ray diffraction, energy dispersive X-rays, differential scanning calorimetry, atomic force microscopy, scanning electron microscopy and transmission electron microscopy techniques have been employed to characterize the synthesized selenium nanoparticles. Gas chromatographic analysis of the reaction mixture established the non-catalytic role of the vinyl monomers, which were found to be consumed during the course of the reaction.

1. Introduction

Nano-materials research received a great deal of interest in recent years because of the outstanding electrical, optical, catalytic and biological properties of the nano-size materials as compared to those of the bulk-materials [1]. An extensive reported literature exists on the synthesis and applications of nanoparticles of both noble metals, such as silver, gold, platinum, etc., and semiconductors, like CdSe, ZnSe, etc. However, research on nano-metalloid, like selenium, is scanty. Nano-selenium is an important semiconductor, with indirect bandgap of 1.6 eV [2,3]. Pure selenium as well as selenium containing materials, such as ZnSe, CdSe, etc., play important role in many applications, because of their photoconductive and photovoltaic properties. Selenium is widely used in the production of photographic exposure meters, photocells, pressure sensors and electrical rectifiers because of its high photoconductivity, and large piezoelectric, thermoelectric, and non-linear responses. The polyvinyl alcohol-stabilized selenium nanoparticles can be efficiently utilized, to produce polymeric films as well as hydrogels containing nano-selenium, which would have many technological applications. Selenium, being an essential micronutrient [4] and an antioxidant, is expected to have enhanced activity in nano-form when stabilized by suitable bio-degradable stabilizers.

Nano-selenium can be produced in various forms, such as nanoplates [2], nanoribbons [3], nanowires [5], nanotubes [6], nanoparticles [7], etc., using different synthetic methods. Laser photolysis and thermolysis of organic selenides [8], thermal chemical vapor deposition [9] methods have been used for the synthesis of elemental selenium. The most frequently used one is reduction method, which includes chemical reduction [10], γ-radiolytic reduction [11], bacterial reduction [12], etc. However, some literature on the formation of nano-selenium via oxidation method, such as reaction of selenourea with hydroxyl radical [13], electrochemical oxidation of selenide [14], etc., also exists. We too have reported the formation of selenium nanoparticles by the oxidation of sodium selenosulphate with acid [7] and acrylonitrile (AN) [15]. With the aim of developing a new simple method, synthesis of selenium nanoparticles has been carried out by the reaction of sodium selenosulphate with different monomers, under ambient conditions.

The synthesized selenium nanoparticles were characterized by UV–vis optical absorption spectroscopy, X-ray diffraction (XRD), energy dispersive X-rays (EDAX), differential scanning calorimetry (DSC), atomic force microscopy (AFM), scanning electron microscopy (SEM) and transmission electron microscopy (TEM) techniques. Gas chromatography was used to understand the role of vinyl monomers in the synthesis.

NMR technique was used to confirm the structure of byproduct.

* Corresponding author. Tel.: +91 22 25593994; fax: +91 22 25505151.
E-mail address: manmoku@barc.gov.in (M. Kumar).

0025-5408/$ – see front matter © 2009 Elsevier Ltd. All rights reserved.
doi:10.1016/j.materresbull.2009.09.001

2. Experimental details

High purity polyvinyl alcohol (PVA) of molecular weight 125,000 and AR grade acrylamide (AM) obtained from S.D. Fine chemical, laboratory grade N,N′-dimethylene bis acrylamide (BisAM) from sigma, methyl methacrylate (MMA) from R. Johnson, acrylic acid from Ferak Berlin and selenium powder from Aldrich, were used as received. All the other chemicals used were of GR grade, procured from the local market. Sodium acrylate (NaA) was prepared by neutralizing acrylic acid monomer with sodium hydroxide, and the final pH of the solution was adjusted to ~8. Aqueous solutions were prepared, using water obtained from Millipore-Q water purification system. Sodium selenosulphate was prepared by the method reported earlier, using reaction between aqueous Na_2SO_3 solution and Se powder [16]

$$Na_2SO_{3(aq)} + Se_{(s)} \rightarrow Na_2SeSO_{3(aq)} \quad (1)$$

Briefly, a mixture of selenium powder (2 g) and solution of Na_2SO_3 (20 g) in 100 ml water was refluxed at 70 °C, for about 7 h. After completion of the refluxing process, the reaction mixture was filtered, and the solution obtained was kept in dark to prevent photo-oxidation. This sodium selenosulphate solution (~0.25 M), containing unreacted Na_2SO_3, was used as a stock for Se precursor. 1% PVA stock solution was prepared by the addition of 1.0 g of PVA into 100 ml water, while stirring at 80 °C. Both these stock solutions were diluted with water, to the required concentrations, for different experiments.

PVA-stabilized Se nanoparticles were synthesized by reaction of sodium selenosulphate (concentration 5×10^{-4} to 1.5×10^{-3} mol dm^{-3}) with different vinyl monomers in aqueous medium, in the presence of PVA as a stabilizer, in the concentration range 0.05–0.15%. The formation of selenium nanoparticles was studied for different time periods, depending on the nature and the concentration of the monomer used. Completion of the reaction, during the study of the reaction kinetics, was checked by spectrophotometric method as well as by the addition of dilute nitric acid in a small volume of the reaction mixture, after separating the selenium nanoparticles, using high-speed centrifuge (acid test). The presence of unreacted sodium selenosulphate was indicated by almost instantaneous development of red colour due to the acid-induced formation of selenium nanoparticles [7].

UV–vis optical absorption spectra of the selenium nanoparticle sols were recorded, using a double beam spectrophotometer, model Spectroscan 2600 from Chemito. XRD patterns of the nanoparticles were recorded with a Phillips X-ray diffractometer, model PW 1710, using a Cu K_α source (λ = 0.15406 nm). DSC measurements were carried out, using a Mettler TA 3000 thermal analysis system. About 5–10 mg of the synthesized selenium nanoparticles and standard selenium powder were weighed into aluminum crucibles separately, and DSC measurements of both the samples were carried out in N_2 atmosphere, at a heating rate of 10 °C/min., from 50 to 250 °C (model DSC-30). Selenium nanoparticles, separated from aqueous sols, using a high-speed centrifuge, at about 15,000 rpm, washed with water and dried at room temperature, were used for XRD and thermal analysis measurements. AFM analysis of the synthesized selenium nanoparticles was carried out, using a Solver P47 model from NT-MDT, Russia. SEM of the synthesized selenium nanoparticle was recorded, using a TESCAN VEGA MV 2300 T/A digital microscope. TEM characterization was carried out with a JEOL-2000 FX electron microscope, using the sample on a copper grid coated with a thin amorphous carbon film. Gas chromatography experiments were carried out on GC 8610 model from Chemito, using a Porapak-Q column of length of 6 ft and diameter of 1/8 in., at 230 °C, and nitrogen, as a carrier gas. NMR spectra of the samples were taken on Bruker machine.

3. Results and discussion

In an attempt to synthesize polymer–selenium nanoparticle composites by radiation-induced method, it was observed that sodium selenosulphate reacts with vinyl monomers, precipitating elemental selenium, under ambient conditions. The simplicity and environmental friendly nature of the reaction drove us to study it in detail, and to develop it as a new method for production of selenium nanoparticles. A detailed study of the reaction was first carried out with acrylamide monomer, in the presence of PVA stabilizer, to produce selenium nanoparticles. Then, it was extended to other vinyl monomers, such as sodium acrylate, N,N′-dimethylene bis acrylamide, methyl methacrylate, α-methyl styrene, etc. PVA was found to be an efficient stabilizer for selenium, as its presence in the reaction mixture resulted in the formation of orange/red coloured selenium nanoparticle sols, while in its absence, black elemental selenium powder precipitated out from the reaction mixture. Kinetics of the formation reaction and particle size of synthesized selenium nanoparticles, by reaction of sodium selenosulphate with different monomers, have been investigated.

The intensity of the selenium nanoparticle sols was found to be dependent on the concentration of sodium selenosulphate taken in the reaction mixture. A typical selenium nanoparticle sol formed by the reaction of 1.0×10^{-3} mol dm^{-3} sodium selenosulphate with 1.6×10^{-2} mol dm^{-3} acrylamide, in the presence of 0.05% PVA is shown in Fig. 1.

Selenium nanoparticles are known to exhibit a regular absorption maximum, in the wavelength region above 350 nm, only when particles size is 150 nm, or more. Both the absorption maximum and the peak intensity are reported to change with the particle size. The absorption maximum generally shifts towards red, and the peak intensity decreases with increase in the size of the nanoparticles [7,17]. Fig. 2 shows the effect of concentration of

Fig. 1. Aqueous selenium nanoparticles sol obtained by the reaction of 1.0×10^{-3} mol dm^{-3} sodium selenosulphate with 1.6×10^{-2} mol dm^{-3} acrylamide in the presence of 0.05% PVA.

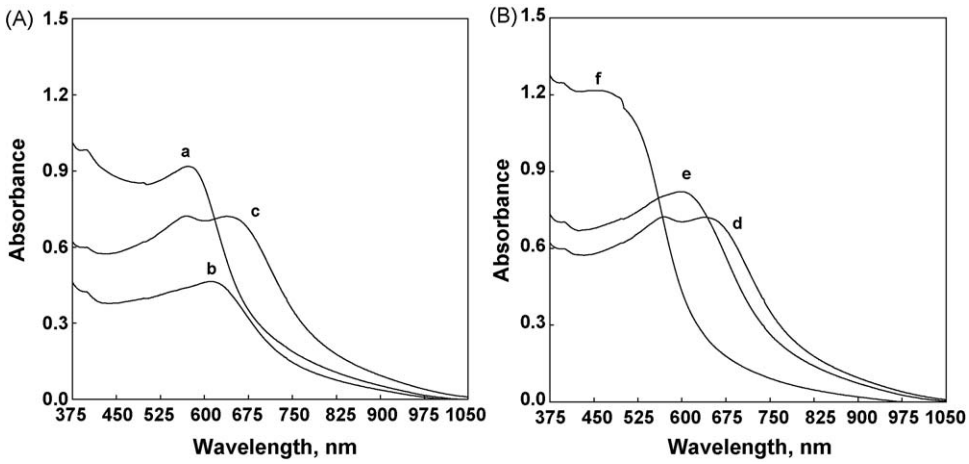

Fig. 2. The effect of (A) sodium selenosulphate concentration, (a) 0.5×10^{-3}, (b) 1.0×10^{-3} and (c) 1.5×10^{-3} mol dm^{-3}, at a fixed PVA concentration of 0.05%, and (B) PVA concentration, (d) 0.05%, (e) 0.10% and (f) 0.15% PVA, at a fixed sodium selenosulphate concentration of 1.5×10^{-3} mol dm^{-3}, on the optical absorption spectrum of selenium nanoparticle sols (recorded at 24 h of reaction time), prepared by reaction with 1.6×10^{-2} mol dm^{-3} acrylamide, in aqueous medium.

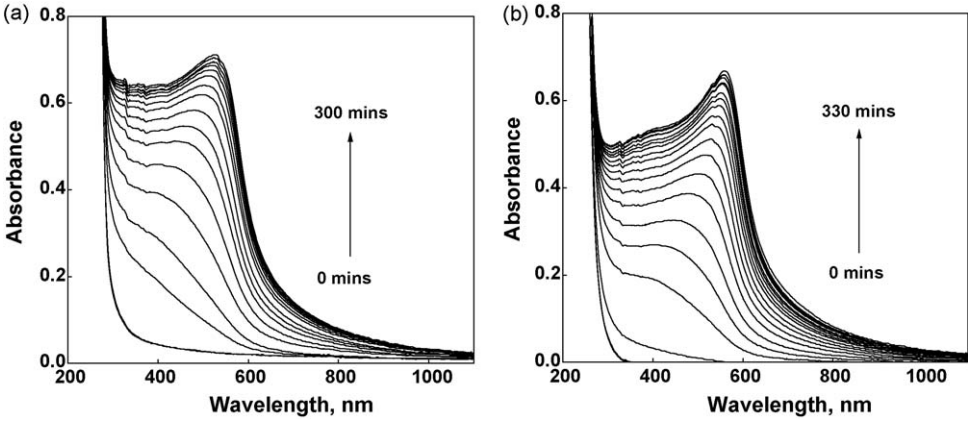

Fig. 3. Development of absorption spectra of the selenium sol, produced by the reaction of 1.5×10^{-3} mol dm^{-3} sodium selenosulphate with 9.0×10^{-2} mol dm^{-3} (a) BisAM and (b) sodium acrylate, in the presence of 0.05% PVA (path length = 2 mm).

the selenium precursor as well as that of PVA on the UV–vis optical absorption spectra of selenium nanoparticle sols (recorded at 24 h of the reaction time), prepared by the reaction of sodium selenosulphate with acrylamide monomer. It is observed that with increase in the sodium selenosulphate concentration from 0.5×10^{-3} to 1.5×10^{-3} mol dm^{-3}, the absorption maximum shifts to higher wavelength, whereas intensity of the absorption band first decreases, and then increases, as shown in Fig. 2A. The presence of an additional absorption band, with maximum at ~570 nm, in the sol formed at the highest studied concentration of sodium selenosulphate, may be due to formation of two types of selenium nanoparticles. The observed increased intensity of this sol may be due to the contribution from these smaller selenium nanoparticles, which are expected to have higher extinction coefficient. However, when the concentration of the PVA stabilizer is varied from 0.05% to 0.15%, at fixed concentrations of sodium selenosulphate and acrylamide monomer, an increase in intensity of the absorption peak, along with a blue shift in its absorption maximum, is observed, as shown in Fig. 2B, suggesting a decrease in the particle size. The observed spectral shifts match well with that reported earlier [7,15,17], due to decrease in the particle size. Thus, it is clear from Fig. 2 that, with increase in the concentration of selenium precursor, size of the nanoparticles increases, whereas the increase in the concentration of PVA stabilizer results in smaller-sized selenium nanoparticles.

Fig. 3a and b show the absorption spectra of the selenium sols, at different times, formed by the reaction of sodium selenosulphate (1.5×10^{-3} mol dm^{-3}) with BisAM and NaA monomer (9.0×10^{-2} mol dm^{-3}), respectively, in the presence of 0.05% PVA. There is a gradual red shift in the absorption maximum with the reaction time, in the case of both the monomers, indicating growth of the nanoparticles. The absorption spectrum of the reaction mixture did not show any change in the studied wavelength region up to about initial 45 min (in the case of BisAM) and 60 min (in the case of NaA) of reaction time, both in air and nitrogen-saturated solutions. Probably, the changes might be taking place in the lower wavelength region.

The nature of the absorption spectrum of the selenium sol was also found to depend on the functional group present in the monomer used. The absorption spectra of selenium sols formed by the reaction of sodium selenosulphate with the different studied monomers, are shown in Fig. 4. These selenium sols have absorption maxima values of 330, 528, 558, 574 and ~560 nm for acrylonitrile, N,N′-dimethylene bis acrylamide, sodium acrylate, acrylamide and methyl methacrylate monomers, respectively, indicating increase in the average size of the selenium nanoparticles in the same order. The lower value of the absorption maximum, in the case of methyl methacrylate, is due to only ~40% completion of the reaction. On comparison of these results with kinetics of the reaction with different monomers (as discussed

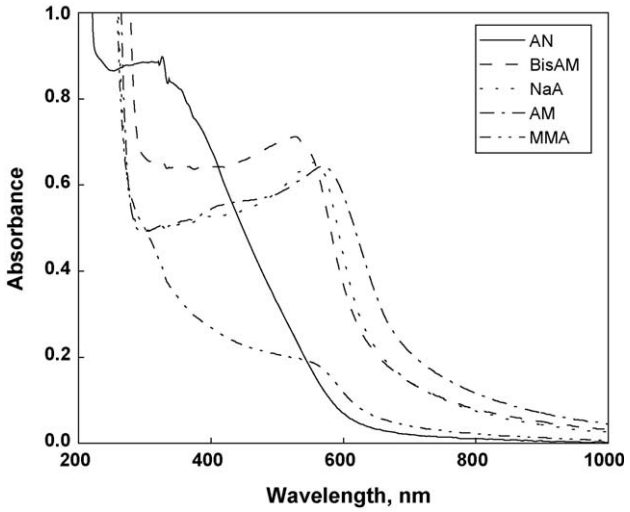

Fig. 4. Absorption spectra of the selenium sols, produced by the reaction of 1.5×10^{-3} mol dm^{-3} sodium selenosulphate with 9.0×10^{-2} mol dm^{-3} of different monomers, in the presence of 0.05% PVA, on about 100% completion of the reactions, except in the case of methyl methacrylate, where the extent of reaction completion was about 40% (optical path length = 2 mm).

subsequently), it can be concluded that, for a given concentration of sodium selenosulphate, the increased rate of reaction, due to either higher concentration of monomer or its reactivity, leads to smaller-sized selenium nanoparticles or vice versa.

Crystal structure of selenium nanoparticles was determined by XRD technique. The typical XRD patterns of the synthesized sample, after heat treatment at 130 °C for 30 min, and that of the commercially available selenium, are displayed in Fig. 5a and b, respectively. The XRD pattern of the synthesized selenium nanoparticles, without heat treatment, was much more noisy, with broader peaks (plot not shown), indicating nano-crystalline nature of the particles. All the diffraction pattern peaks could be indexed according to trigonal phase, with lattice constants $a = 4.366$ Å and $c = 4.956$ Å, which match very well with the reported values (JCPDS FILE No., 06-362).

Further, chemical composition of the synthesized selenium nanoparticles was also confirmed by EDAX. The EDAX spectrum of the nanoparticles, shown in Fig. 6, also indicates that the nanoparticles are of pure selenium only, and no other element is present therein.

DSC thermograms of the synthesized selenium nanoparticles and standard commercial selenium sample were recorded from 50 to 250 °C. DSC thermogram of the synthesized selenium nanoparticles showed an exothermic transition at 85 °C, along with endothermic melting peak at 217 °C (Fig. 7a). Enthalpy of the transition was found to be 21.83 J/g. The repeat DSC thermogram of the same selenium sample, recorded after bringing it to ambient temperature, did not show any exothermic peak at the mentioned temperature (plot not shown). This clearly indicates that the selenium particles loose their nano-crystalline nature in the first thermal run itself, and the transition could be assigned to increase in crystallinity of the selenium nanoparticles. This observation is in corroboration with the XRD results obtained with the synthesized sample and that annealed at 130 °C. DSC thermogram of the standard selenium powder sample, depicting melting peak 217 °C, without any such exothermic peak, is shown in Fig. 7b.

AFM, SEM, and TEM are very important techniques, which are used to get the information about particle size, shape, surface topography, etc. Therefore, morphology and structure of the synthesized selenium nanoparticles were also investigated by these techniques. Typical 2D and 3D AFM images of the synthesized selenium nanoparticles are shown in Fig. 8. The 2D image of the synthesized selenium nanoparticles shows that the average size of the selenium nanoparticles, or that of their aggregates, is about 100 nm. While the 3D image indicates the presence of individual spherical particles, with maximum height of 8 nm in the *z*-direction. Thus, it can be concluded from these results that, some selenium particles, with size almost an order of magnitude smaller, are also formed, along with the bigger nanoparticles, or nano-aggregates of size about 100 nm.

Scanning electron microscope and transmission electron microscope images of the synthesized selenium nanoparticles are shown in Fig. 9a and b, respectively. Spherical shape of the individual nanoparticles and narrow size distribution (with average size about 100 nm) are evident from both SEM and TEM images. The conclusion drawn from AFM, SEM and TEM studies are more or less in corroboration with each other. Thus, the present method is capable of producing spherical selenium nanoparticles. However, size of the particles (100–200 nm) and kinetics of the formation process depend upon the nature and concentration of the monomer used, as discussed later. The size of the selenium nanoparticles produced by reaction of sodium selenosulphate with acrylamide monomer (~100 nm) is larger than that of those formed by reaction with acrylonitrile (~70 nm), under similar experimental conditions [15].

The rate of formation of selenium nanoparticles was found to be dependent on the nature as well as concentration of the vinyl monomer used in the reaction. When the reaction was carried out at higher concentration of the monomers, selenium was released

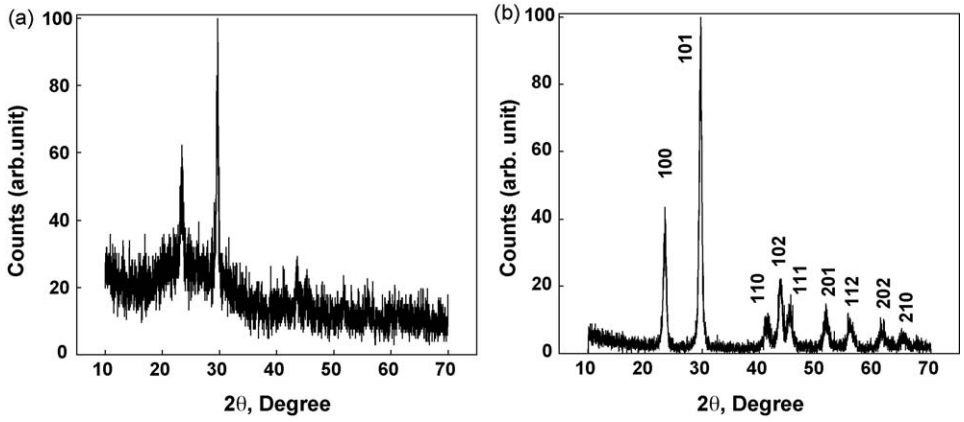

Fig. 5. XRD pattern of (a) the synthesized selenium nanoparticles annealed at 130 °C for 30 min and (b) commercial selenium sample. Selenium nanoparticles were synthesized by the reaction of 1.5×10^{-3} mol dm^{-3} sodium selenosulphate with 1.6×10^{-2} mol dm^{-3} acrylamide, in the presence of 0.05% PVA.

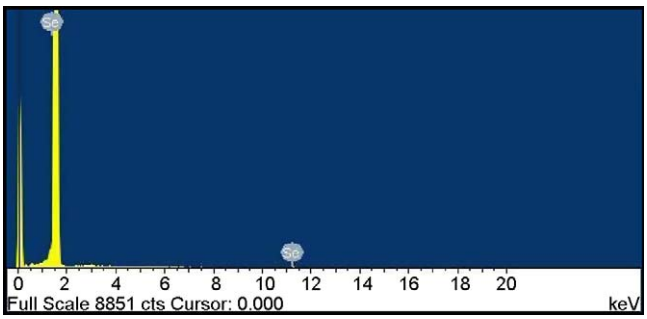

Fig. 6. EDAX pattern of the selenium nanoparticles synthesized by the reaction of 1.5×10^{-3} mol dm^{-3} sodium selenosulphate with 1.6×10^{-2} mol dm^{-3} acrylamide, in the presence of 0.05% PVA.

from sodium selenosulphate at much faster rate than that at lower concentration of the monomers. Kinetics of the reaction was studied with acrylamide, sodium acrylate, BisAM and methyl methacrylate monomers, and was also compared with our earlier reported results with acrylonitrile monomer [15]. The reaction with acrylic acid monomer was not studied, as the presence of –COOH group leads to acid-induced selenium formation, in addition to that due to carbon–carbon double bond present in it. In a typical solution, containing 9.0×10^{-2} mol dm^{-3} acrylamide, 1.5×10^{-3} mol dm^{-3} sodium selenosulphate and 0.05% PVA, appearance of the selenium nanoparticles was observed in 85 min (as measured by the UV–vis spectrophotometer), and the reaction was completed in ~6 h, as confirmed by both UV–vis spectrophotometer, and absence of sodium selenosulphate by the acid test [7]. Table 1 lists the time for the appearance of the colour due to the selenium nanoparticle formation and the time for completion of the reaction, at fixed concentrations of sodium selenosulphate, 1.5×10^{-3} mol dm^{-3} and PVA, 0.05%, while varying concentrations of the different monomers. These timings being indicator of the rate of the reaction can be used to compare kinetics of the reaction under different conditions.

In our previous study [15], formation of elemental selenium by the reaction of sodium selenosulphate with acrylonitrile was found to be faster as compared to that observed with the vinyl monomers in the present study. The increase in reaction time may be because of less reactivity of the monomers due to different functional groups present therein, as compared to that in acrylonitrile, containing nitrile functional group. It is clear from the results in Table 1 that the rates of the reaction of sodium selenosulphate with different monomers, in decreasing order, are as follows

$$\text{Rate}_{(AN)} > \text{Rate}_{(BisAM)} \approx \text{Rate}_{(NaA)} > \text{Rate}_{(AM)} > \text{Rate}_{(MMA)}$$

The observed reactivity can be correlated with the presence of different functional groups in the monomers. As reported in our earlier study with acrylonitrile monomer [15], the reaction takes place via a four-membered cyclic ring intermediate, formed by nucleophilic attack of anionic selenium on β-carbon of the monomer, followed by release of selenium, as shown in Scheme 1. Formation of the product was also confirmed by NMR technique, after separating it from the reaction mixture, in the case of reaction with acrylonitrile monomer. Fig. 10a and b shows NMR spectra of the acrylonitrile and product isolated from the reaction mixture,

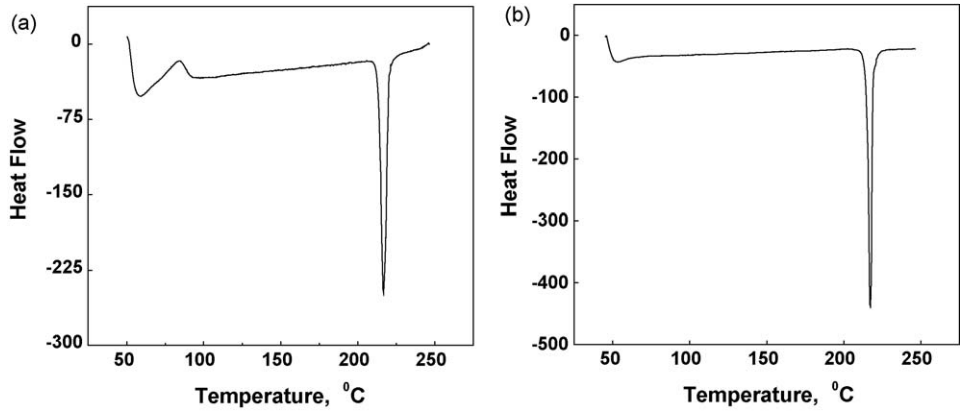

Fig. 7. DSC thermogram of (a) the selenium nanoparticles synthesized by the reaction of 1.5×10^{-3} mol dm^{-3} sodium selenosulphate with 1.6×10^{-2} mol dm^{-3} acrylamide, in the presence of 0.05% PVA and (b) standard commercial selenium sample.

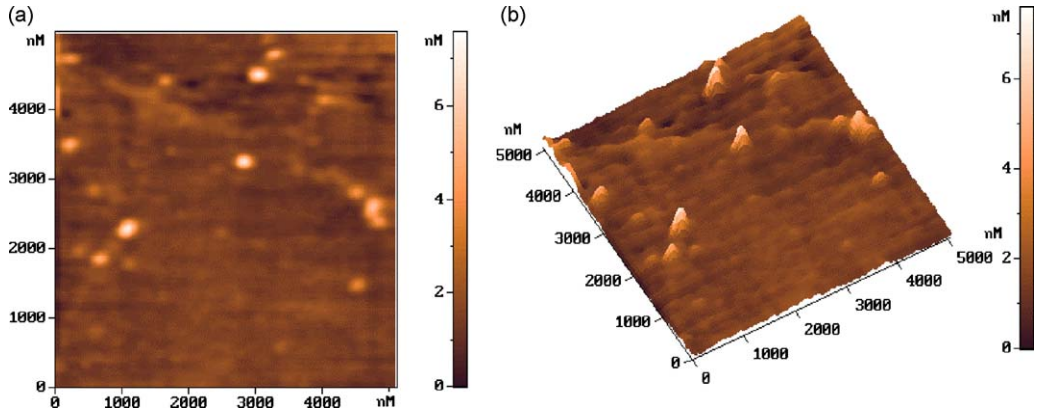

Fig. 8. AFM images of the selenium nanoparticles formed by the reaction of 1.5×10^{-3} mol dm^{-3} sodium selenosulphate with 1.6×10^{-2} mol dm^{-3} acrylamide, in the presence of 0.05% PVA: (a) 2D image and (b) 3D image.

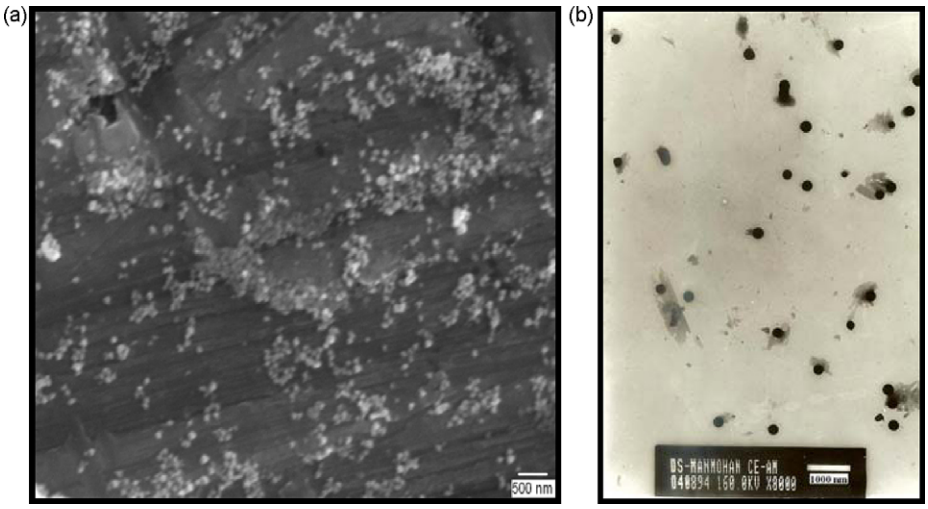

Fig. 9. (a) SEM and (b) TEM images of the selenium nanoparticles formed by the reaction of 1.5×10^{-3} mol dm^{-3} sodium selenosulphate with 1.6×10^{-2} mol dm^{-3} acrylamide, in the presence of 0.05% PVA.

respectively. The peaks for three sp^2 hybridized proton of acrylonitrile appear in between δ5.5 and δ6.5 ppm, as shown in Fig. 10a. The observed triplet–triplet pattern is due to saturation of carbon–carbon double bond of acrylonitrile monomer during the reaction which leads to four sp^3 hybridized protons appearing between δ2.5 and δ3.0 ppm. Since, the product was isolated from alkaline medium, the peak for–OH group was not observed, as it was ionized to its sodium salt. The observed peak at δ4.7 ppm is due to water.

In the case of acrylamide, the gas chromatographic analysis of the reaction mixture, after separating the selenium nanoparticles by high-speed centrifuge, showed decrease in monomer concentration as the reaction progressed, but no new product was seen up to the studied retention time of about 45 min. This observation ruled out the possibility of the monomer acting as a catalyst, in the reaction. A strong electron withdrawing group, like nitrile, as in the case of acrylonitrile, will reduce electron density at carbon–carbon double bond of the monomer, hence facilitating nucleophilic attack of anionic selenium on to it. Whereas, the presence of electron donating group, such as methyl, as in the case of methyl methacrylate, increases electron density at the carbon–carbon double bond, and hence will retard the nucleophilic attack. Resonance stability of carboxylate anion present in the case of sodium acrylate monomer may be responsible for its higher reactivity. In the case of bis acrylamide monomer, the presence of two carbon–carbon double bonds makes it more reactive than acrylamide monomer.

The formation of selenium nanoparticles was also observed with α-methyl styrene monomer. However, the rate was found to be much slower, requiring more than a week for the formation of selenium. This is because of limited solubility of α-methyl styrene

Table 1
The effect of concentration of different monomers on the kinetics of selenium nanoparticle formation at fixed sodium selenosulphate (1.5×10^{-3} mol dm^{-3}) and PVA (0.05%) concentrations.

Monomer	Concentration (mol dm^{-3})	Reaction time[a] (min)	Time to complete the reaction (min)
Acrylonitrile[b]	10×10^{-3}	[c]	–
	50×10^{-3}	30	–
	90×10^{-3}	15	<60
	141×10^{-3}	07	–
N-N′-dimethylene bis acrylamide	10×10^{-3}	[c]	–
	50×10^{-3}	105	–
	90×10^{-3}	45	~300
	141×10^{-3}	45	–
Sodium acrylate	10×10^{-3}	[c]	–
	50×10^{-3}	[c]	–
	90×10^{-3}	70	~330
	Sat. solution	45	–
Acrylamide	10×10^{-3}	[c]	–
	50×10^{-3}	210	–
	90×10^{-3}	85	~360
	141×10^{-3}	70	–
Methyl methacrylate	10×10^{-3}	[c]	–
	50×10^{-3}	[c]	–
	90×10^{-3}	330	>8 h
	141×10^{-3}	295	–

[a] Reaction time to observe colour changes, as monitored by UV–vis spectrophotometer.
[b] Ref. [15].
[c] Reaction was not observed up to ~9 h.

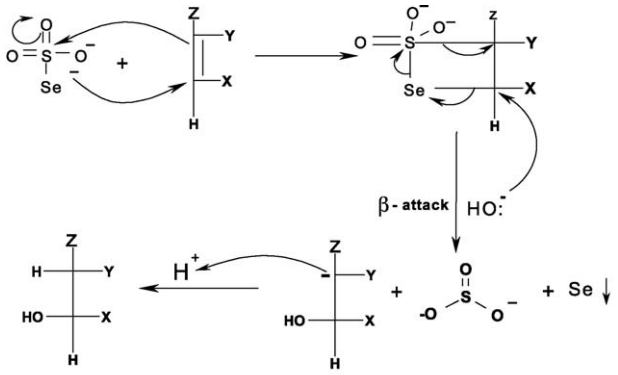

where,

Name of the Monomer	X	Y	Z
Acrynonitrile	-H	-H	-CN
Sodium acrylate	-H	-H	-COONa
N,N'-dimethylene bis acrylamide	-H	-H	-CONH-CH_2-NH-CO-CH=CH_2
Acrylamide	-H	-H	-$CONH_2$
Methyl Methacrylate	-H	-CH_3	-$COOCH_3$

Scheme 1. General mechanism for the formation of selenium by the reaction of sodium selenosulphate with different monomers.

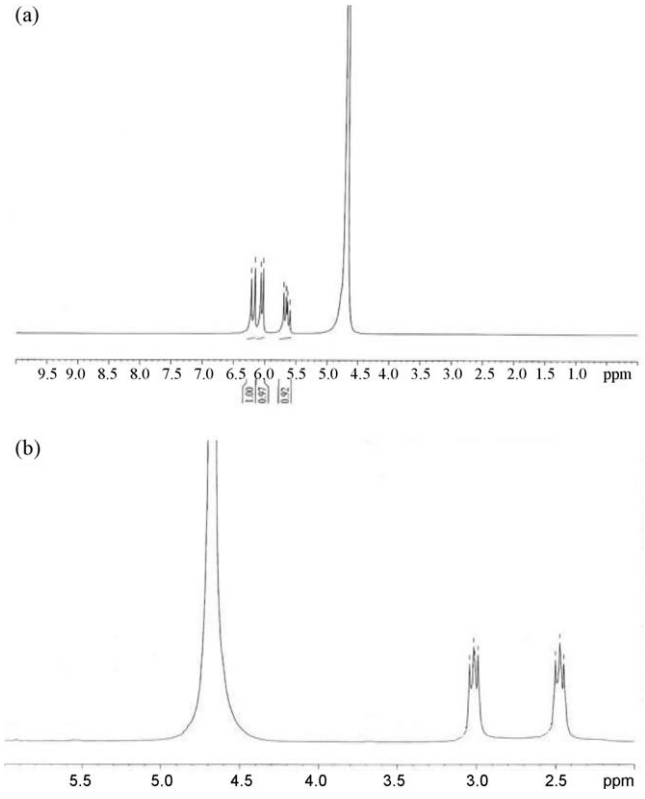

Fig. 10. NMR spectra of (a) acrylonitrile and (b) product of the reaction mixture.

in aqueous medium as well as due to the presence of electron donating methyl group on carbon–carbon double bond. Thus, we can say that, ''the higher is the electron withdrawing capacity of the substituent at the carbon–carbon double bond of the vinyl monomers, the faster is the reaction, or vice versa''.

4. Conclusions

Vinyl monomers-induced synthesis of selenium nanoparticles has been found to be a simple and convenient method, which can be carried out under ambient conditions. PVA was used as a stabilizer for the selenium nanoparticles. The size of the selenium particles was found to increase with sodium selenosulphate concentration as well as with aging of the sols. Whereas higher concentration of PVA favoured the formation of smaller selenium nanoparticles. The functional group present in the monomers influenced both, the reaction rate and size of the resultant nanoparticles. Nano-nature of the synthesized selenium particles and increase in their crystallinity on heating, were confirmed by both, XRD and DSC experiments. Spherical selenium nanoparticles of the size about 100 nm, as determined by AFM, SEM and TEM techniques, could be produced. The selenium nanoparticles may serve as template, to generate other important nano-materials, and find applications in fabrication of nanoscale optoelectronic devices.

Acknowledgements

The author Chetan P Shah is grateful to Department of Atomic Energy, for awarding research fellowship. The authors are thankful to Dr. P.A. Hassan, BARC, for AFM, Dr. S.K. Gupta, BARC, for SEM and EDAX, Dr. D. Shrivastava, BARC, for TEM, and Dr. L. Varshney, BARC, for DSC experiments. The authors also wish to acknowledge Dr. T. Mukherjee and Dr. S.K. Sarkar, for their encouragement during the course of the study.

References

[1] S. Nath, S.K. Ghosh, T. Pal, Chem. Commun. (2004) 966.
[2] Y. Haoyong, X. Zhude, B. Huahui, B. Jingyi, Z. Yifan, Chem. Lett. 34 (2005) 122.
[3] X. Cao, Y. Xie, S. Zhang, F. Li, Adv. Mater. 16 (2004) 649.
[4] M.A. Bakir, G. Alya, A. Mohammad, R. Azroony, F. Kasies, J. Radioanal. Nucl. Chem. 266 (2005) 165.
[5] B. Zhang, X. Ye, W. Dai, W. Hou, F. Zuo, Y. Xie, Nanotechnology 17 (2006) 385.
[6] L. Peng, M. Yurong, C. Weiwei, W. Zhenzhong, W. Jian, Q. Limin, C. Dongmin, Nanotechnology 17 (2007) 205704.
[7] C.P. Shah, M. Kumar, P.N. Bajaj, Nanotechnology 18 (2007) 385607.
[8] J. Pola, A. Ouchi, Molecules 14 (2009) 1111.
[9] S.N. Yannopoulos, K.S. Andrikopoulos, J. Chem. Phys. 121 (2004) 4747.
[10] L. Qing, W-W.Y. Vivian, Chem. Commun. (2006) 1006.
[11] Z. Yingjie, Q. Yitai, H. Huang, Z. Manwei, Mater. Lett. 28 (1996) 119.
[12] R.S. Oremland, M.J. Herbel, J.S. Blum, S. Langley, T. Beveridge, P.M. Ajayan, T. Sutto, A.V. Ellis, S. Curran, Appl. Environ. Microbiol. 70 (2004) 52.
[13] B. Mishra, P.A. Hassan, K.I. Priyadarsini, H. Mohan, J. Phys. Chem. B 109 (2005) 12718.
[14] T.C. Franklin, W.K. Adeniyi, R. Nnodimele, J. Electrochem. Soc. 137 (1990) 480.
[15] C.P. Shah, K.K. Puspa, M. Kumar, P.N. Bajaj, Cryst. Growth Des. 8 (2008) 4159.
[16] S. Gorer, G. Hodes, J. Phys. Chem. 98 (1994) 5338.
[17] Z.H. Lin, C.R.C. Wang, Mater. Chem. Phys. 92 (2005) 591.